arXiv:1405.3048v1 [cond-mat.supr-con] 13 May 2014

Magnetism and superconductivity in $Sr_2VFeAsO_3$ revealed by ^{75}As- and ^{51}V-NMR under elevated pressures

Keiji Ueshima[1], Fei Han[2,3], Xiyu Zhu[2,3], Hai-Hu Wen[2,3], Shinji Kawasaki[1], and Guo-qing Zheng[1,2]

[1]*Department of Physics, and Research Center of New Functional Materials for Energy Production, Storage and Transport, Okayama University, Okayama 700-8530, Japan*

[2]*Beijing National Laboratory for Condensed Matter Physics, Institute of Physics, Chinese Academy of Sciences, Beijing 100190, China and*

[3]*Center for Superconducting Physics and Materials, National Laboratory of Solid State Microstructures and Department of Physics, Nanjing University, Nanjing 210093, China*

(Dated: May 14, 2014)

Abstract

We report ^{75}As- and ^{51}V-nuclear magnetic resonance (NMR) measurements on the iron-based superconductor $Sr_2VFeAsO_3$ with alternating stacks structure. We find that the ^{75}As nuclear spin-spin relaxation rate ($1/T_2$) shows a pronounced peak at $T_N = 165$ K, below which the resonance peak shifts to a higher frequency due to the onset of an internal magnetic field. The ^{51}V spectrum does not shift, but is broadened below T_N. We conclude that the Fe electrons oder antiferromagnetically below T_N with a magnetic moment $m_{Fe} \sim 0.4\ \mu_B$. Application of external pressure up to 2.4 GPa reduces T_N in a rate of -40 K/GPa, and enhances the superconducting transition temperature T_c in a rate of 2 K/GPa. The pressure-temperature phase diagram for $Sr_2VFeAsO_3$ shows that superconductivity coexists with antiferromagnetism over a wide pressure range with an unprecedented high T_c up to 36.5 K.

I. INTRODUCTION

The discovery of superconductivity in iron-pnictide $LaFeAsO_{1-x}F_x$ at the superconducting transition temperature $T_c = 26$ K[1] has generated much interest, and led to the discovery of many other families.[2–9] The parent compounds are metallic and show a tetragonal to orthorhombic structural phase transition followed by an antiferromagnetic order. Superconductivity appears after suppressing these orders by electron/hole doping to the FeAs layer, and/or by applying pressure.[10–12] Experiments have suggested that the superconductivity may be related to the quantum critical fluctuations associated with the above-mentioned orders.[13–17]

Recently, high-T_c superconductivity was found in $Sr_2VFeAsO_3$ that composes of alternating stacks of FeAs and perovskite Sr_2VO_3 layers.[18] The $T_c^\rho = 37$ K was inferred from the electrical resistivity measurement, and $T_c^\chi = 32$ K from the magnetic susceptibility. Hereafter in this paper, the T_c refers to T_c^χ. It was reported that T_c increases to 43 K at a pressure $P = 4$ GPa.[19] As in the cuprate high-T_c superconductors, this opens a new gateway to studying the relationship between crystal structure and superconductivity, and has triggered the synthesis of other compounds with similar stacking structures.[20,21] It is interesting that the superconductivity in $Sr_2VFeAsO_3$ is realized without doping by element substitution. Since most stoichiometric Fe-based compounds host magnetism, searching for a possible magnetic order in $Sr_2VFeAsO_3$ has also become an important subject.[22]

Indeed, previous magnetic susceptibility and specific heat found an anomaly at a high temperature $T_M \sim 150$ K, which was ascribed to a possible magnetic transition.[22] Since the Fe Mössbauer spectra showed no additional broadening below T_M, it was proposed that the anomaly originates from the V spin ordering.[22] However, the reported Fe Mössbauer spectra split into two peaks even above T_M,[22] and the reported full width at the half maximum (FWHM) of the Mössbauer spectra is rather comparable with that observed in the Fe ordered state of non-doped $BaFe_2As_2$[23] and LaFeAsO.[24] This suggests that it is difficult to rule out Fe spin order by the Mössbauer measurement, and the origin of the anomalies at $T_M \sim 150$ K in $Sr_2VFeAsO_3$ remains unclear. It is important to elucidate whether the anomaly is due to a magnetic order, and whether the Fe electrons or V electrons order. This is because the relationship between magnetism and superconductivity is an important issue generally in strongly-correlated electron systems.

In this paper, we report ^{75}As- and ^{51}V-NMR studies on polycrystalline $Sr_2VFeAsO_3$ under elevated pressures. Since $Sr_2VFeAsO_3$ is a stoichiometric compound, we use external pressure to tune the electronic state. We have constructed a pressure-temperature phase diagram that shed lights on the relationship between magnetism and superconductivity in this system.

We found an internal magnetic field H_{int} = 1.1 T at the As site, while the ^{51}V-NMR spectrum is broadened due to a field distribution of 0.005 T below T_N = 165 K. The ^{75}As spin-spin relaxation rate ($1/T_2$) shows a pronounced peak at T_N. We conclude that it is the Fe electrons that order below T_N, which produces a large internal magnetic field at the As site and a field distribution at the V site, since V is far away from Fe in the unit cell. In the superconducting state, the spin-lattice relaxation rate $1/T_1$ decreases rapidly below T_c as in other pnictides.[14–17,26,27] Thus superconductivity coexists with magnetism in $Sr_2VFeAsO_3$ as in other systems,[13,25] but with a much higher T_c of 36.5 K.

II. EXPERIMENTAL

Polycrystalline samples of $Sr_2VFeAsO_3$ were synthesized by using a two-step solid-state reaction method.[18] First, SrAs powders were obtained by the chemical reaction method with Sr pieces and As grains. Then, they were mixed with V_2O_5 (3N), SrO (2N), Fe and Sr powders (3N), in the formula $Sr_2VFeAsO_3$, ground and pressed into a pellet shape. The weighing, mixing, and pressing process were performed in a glove box with a protective argon atmosphere (the H_2O and O_2 contents were both below 0.1 ppm). The pellets were sealed in a silica tube with 0.2 bar of Ar gas and followed by a heat treatment at 1150 °C for 40 h. Then it was cooled down slowly to room temperature. The transport and magnetic properties were described previously[18]. A large pellet ($\sim$ 1000 mg) was crushed into coarse powder for NMR measurements.

The ac susceptibility measurements using the *in-situ* NMR coil at zero magnetic filed indicates T_c = 32 K. ^{75}As and ^{51}V-NMR measurements were carried out by using a phase-coherent spectrometer. The NMR spectrum is obtained by integrating the spin echo intensity by changing the resonance frequency (f) at a fixed magnetic field of 12.951 T. The T_1 was measured by using a single saturating pulse, and is determined by fitting the recovery curve of the nuclear magnetization to the theoretical function ; $(M_0 - M(t))/M_0 = 0.9\exp(-t/T_1)$

+ 0.1exp($-6t/T_1$), where M_0 and $M(t)$ are the nuclear magnetization in the thermal equilibrium and at a time t after the saturating pulse. The spin-spin relaxation rate ($1/T_2$) was obtained from the relation of the spin echo intensity $I(\tau) = I(0)\exp(-2\tau/T_2)$ where τ is the time separation between the $\pi/2$ and π pulses. Both T_1 and T_2 were measured at the spectra peak corresponding to $H//ab$ configuration.

The pressure was applied by utilizing a NiCrAl/BeCu piston-cylinder type cell filled with silicon oil[28] as the pressure-transmitting medium. The pressure at low temperatures was determined from the T_c values of Sn metal measured by a conventional four-terminal method. The pressure distribution ΔP at low temperatures due to solidification of pressure transmitting media for present cell is quantitatively determined to be 5%.[29]

III. RESULTS

A. Magnetic order probed by ^{75}As and ^{51}V-NMR

First, we show evidence for Fe magnetic order from ^{75}As-NMR and ^{51}V-NMR. Figure 1 shows the typical ^{75}As NMR spectra for the central transition ($m = 1/2 \leftrightarrow$ -1/2 transition). The total nuclear spin Hamiltonian is written as $\mathcal{H} = \mathcal{H}_z + \mathcal{H}_Q$, where $\mathcal{H}_Z = \gamma\hbar\overrightarrow{I} \cdot (\overrightarrow{H_0} + \overrightarrow{H}_{int})$, and $\mathcal{H}_Q$ is due to the interaction between the nuclear quadrupole moment and the electric field gradient (EFG). H_{int} is a local magnetic field due to the hyperfine interaction, and H_0 is the applied magnetic field. The sizable $\mathcal{H}_Q$ for ^{75}As whose nuclear spin is I=3/2 has a large perturbation effect on the $m = 1/2 \leftrightarrow$ -1/2 transition[30]. Since the crystalline axis in a powdered sample is randomly distributed, the NMR spectrum shows a powder pattern depending on the angle θ between the principal axes of the EFG (z') and the external magnetic filed (z).[30] For the case of the As site in the FeAs layer, z' corresponds to the crystal c direction.

As seen in Fig. 1, there is a two-horns shape in the frequency dependence of the spectrum. These two horns (peaks) correspond to $\theta = 41.8°$ (peak at lower frequency) and $\theta = 90°$ i.e. $H_0//ab$ (peak at higher frequency). We are the first to observe the NMR spectra around $T \sim$ 150 K, while previous As-NMR attempt failed to detect a signal around this temperature.[19] We find that the spectrum shifts to a higher frequency below $T_N = 165$ K. The frequency shift of the $\theta = 90°$ peak indicates the appearance of an internal field.

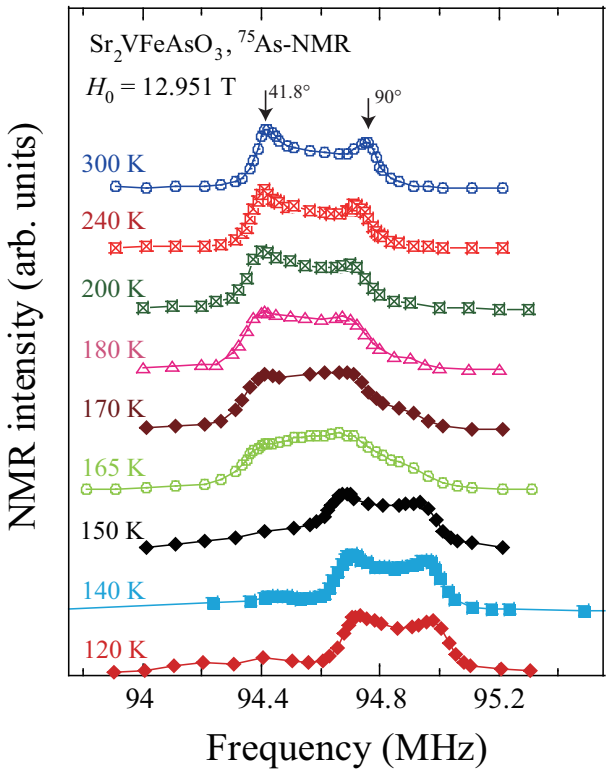

FIG. 1: (color online) Temperature dependence of the frequency swept ^{75}As-NMR spectra (center transitions only) at the fixed magnetic field of $H_0 = 12.951$ T. The two horns correspond to $\theta = 41.8°$ and 90° ($H_0 \parallel ab$-plane), see text for detail.

In contrast, the ^{51}V-NMR spectrum does not shift, while it is broadened below $T_N = 165$ K, as seen in Fig. 2(a). As seen in the figure, we observed a single peak. Since the nuclear spin for V nucleus is $I = 7/2$, this suggests that the EFG is small, if any, at the V site. The spectrum can be fitted by a single Lorentzian curve. As plotted in Fig. 2(b), the FWHM of the ^{51}V-NMR spectrum is increased below $T_N = 165$ K. At T=100 K, the broadening is equivalent to a field distribution of ~ 0.005 T.

The appearance of the internal magnetic field at the As site and a magnetic field distribution at the V site is due to a magnetic order, which is corroborated by the spin dynamics. Figure 3(a) shows the temperature dependence of $1/T_2$, which exhibits a pronounced peak at T_N. Such a peak in a temperature dependence of $1/T_2$ is a characteristic feature of a magnetic order,[32] since $1/T_2$ probes the longitudinal fluctuating field. At the V site, however, $1/T_2$ shows no anomaly at T_N.

The results are consistent with the Fe electrons ordered magnetically below T_N. Namely,

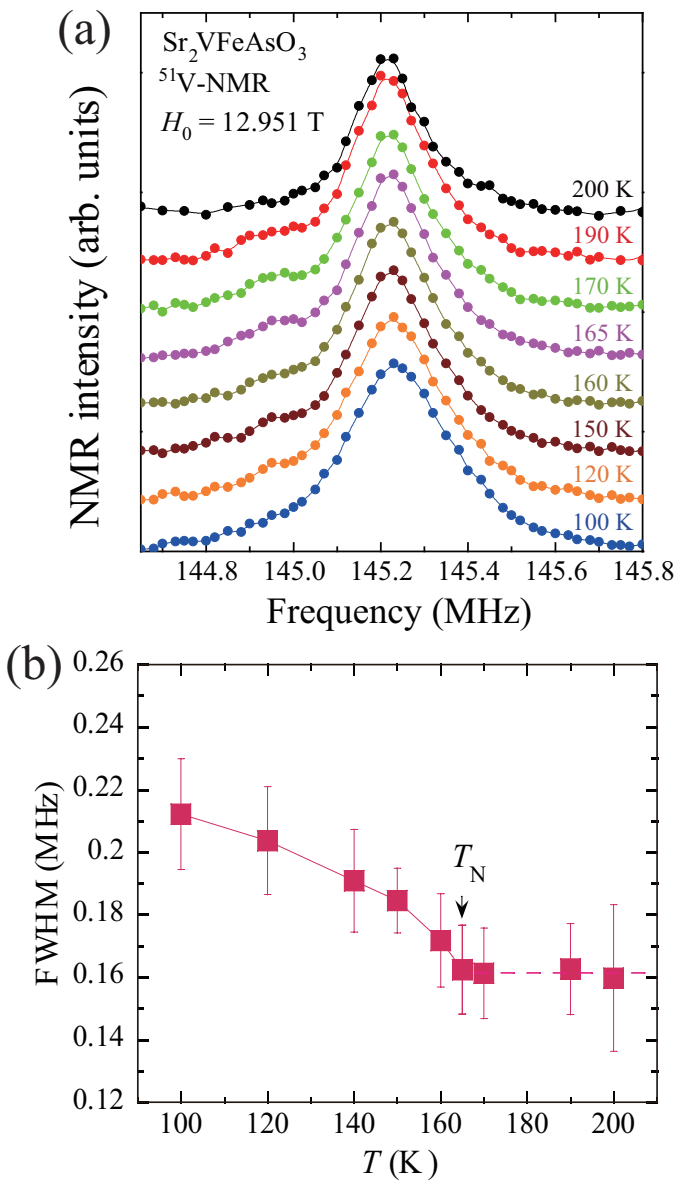

FIG. 2: (color online) (a) Temperature dependence of the frequency swept ^{51}V-NMR spectra at the fixed magnetic field of 12.951 T. (b) Temperature dependence of the full width at the half maximum (FWHM).

the ordered Fe electrons produce an internal magnetic field at the As site through the Fe-3d and As-2p orbital mixing, and create a field distribution at the V site since V is far away from Fe in the unit cell. Assuming the same Fe spin alignment as in LaFeAsO,[24] the effective field at the As site when the external field is applied along the a-axis is given by $H_{eff} = \sqrt{H_0^2 + H_{int}^2}$, where H_{int} is the internal field produced by the ordered Fe spins.[25,31] The

calculated $H_{int}(T)$ and the estimated m_{Fe} using the hyperfine coupling constant ${}^{75}A_{hf}^{\perp} = 2.64$ T/μ_B[31] are plotted in Fig. 3(b). The saturated values $m \sim 0.4$ μ_B is comparable to that observed in non-doped $BaFe_2As_2$[33] and LaFeAsO.[34] Furthermore, a field distribution at the V site due to a dipole-dipole interaction from the Fe spins (s_j), $\Delta H_d = \sum_j \{\frac{3(s_j \cdot r_j)}{r_j^5} - \frac{s_j}{r_j^3}\}$, is calculated to be $\sim$0.004 T at the V site, which is in reasonable agreement with the observed ΔH. Thus, we conclude that the Fe electrons order antiferromagnetically in $Sr_2VFeAsO_3$, as in other iron pnictides.

The transition temperature $T_N = 165$ K found in the present sample is slightly higher than $T_M \sim 150$ K seen in the susceptibility and specific measurements.[22] This is probably due to a difference in the sample quality. In fact, inspection of the derivative of the resistivity data for our sample shows an anomaly at $T_N \sim 165$ K, being consistent with the NMR results. The sample dependence of a putative magnetic transition was reported previously by various measurements.[35,36] For example, μSR(Ref.[35]) and neutron scattering measurements (Ref.[36]) on a sample with lower $T_c \sim 25$ K found an anomaly at a rather lower $T_M \sim 40$ K. The sample difference is likely due to the deficiency of oxygen. When oxygen is deficient, T_c is reduced.[37]

B. Temperature - Pressure phase diagram

Next we present the magnetic and superconducting properties in $Sr_2VFeAsO_3$ under high pressures. Figure 4 shows the temperature dependence of the ac-susceptibility under pressure measured using the *in-situ* NMR coil. The superconducting transitions are clearly seen as rapid decreases of the susceptibility. The $T_c(P)$ are 32 K, 36 K, and 36.5 K at $P =$ 0, 1.9 and 2.4 GPa, respectively. The T_c increases in a rate of 2 K/GPa, which is consistent with previous resistivity measurement under pressure.[19]

Figure 5 shows the temperature dependence of $1/T_2$ at $P = 0$, 1.9, and 2.4 GPa, respectively. Since the sample space in the pressure cell is limited, we can only use a very small amount of sample and as a result, the NMR signal to noise ratio is much smaller compared to the measurement at ambient pressure. It becomes difficult to measure the whole spectra at each temperature around T_N. Therefore we adapt the T_2 measurement to probe the magnetic transition at high pressures. Even so, the fast spin - spin relaxation around T_N results in a rapid decay of the spin echo, and thus a poor S/N. At ambient pressure, we

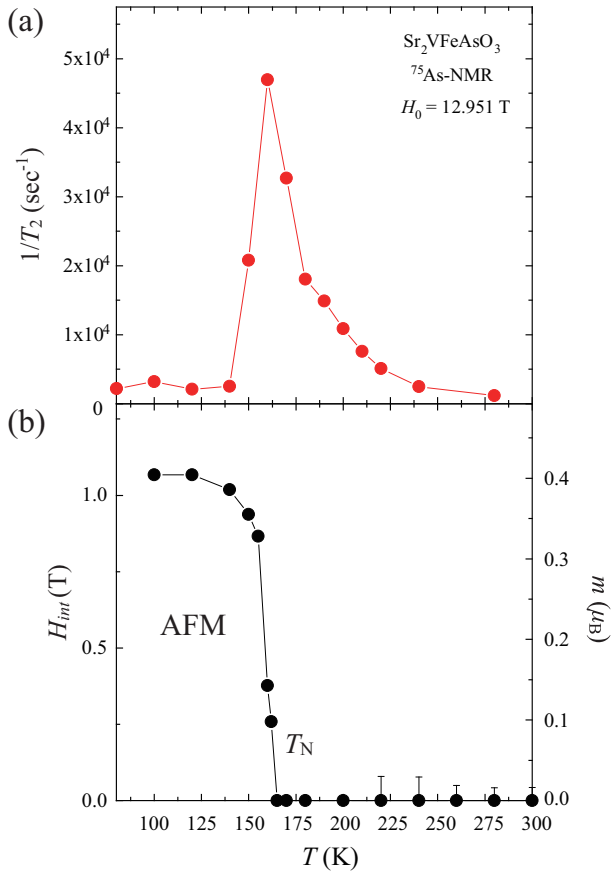

FIG. 3: (color online) (a) Temperature dependence of ^{75}As spin-spin relaxation rate. (b) Temperature dependence of the internal magnetic field (H_{int}) (left vertical axis) deduced from frequency shift of NMR spectra in Fig. 1, and the estimated Fe moment (right vertical axis).

managed to observe the signal around T_N, but this becomes impossible at high pressure because of the small sample amount. Nonetheless, a clear shift of the data points towards lower temperature can be seen. We estimated T_N by extrapolating the data above and below $T_N(P)$, and obtained $T_N(P) = 90$ K $\pm$ 15 K (1.9 GPa) and 70 K $\pm$ 10 K (2.4 GPa) from the intersection of the extrapolated curves. The error bar corresponds to the half of the temperature interval between which we lost the signal. The T_N is reduced by pressure in a rate of -40 K/GPa, which is larger than the cases of $SrFe_2As_2$ (-25 K/GPa)[38] and $LaFeAsO_{0.945}F_{0.055}$ (-17 K/GPa)[39].

As seen in Fig. 6, in the superconducting state below T_c, $1/T_1$ decreases without a Hebel-Slichter peak as in other iron pnictide superconductors.[14–17,26,27] Since T_1 was measured at the peak corresponding to $\theta = 90°$ which experiences an internal magnetic

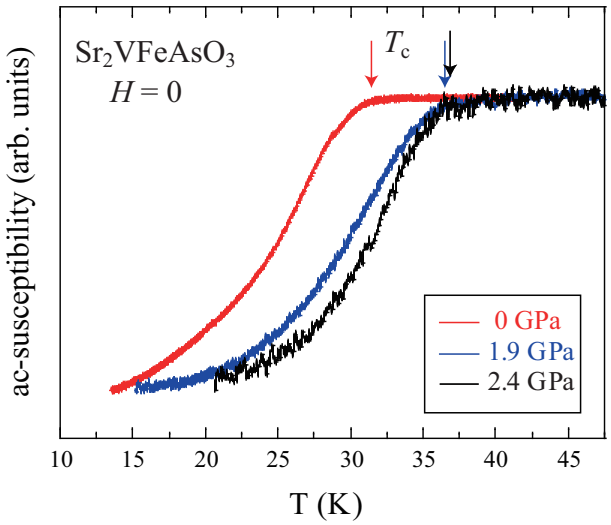

FIG. 4: (color online) The ac-susceptibility for $Sr_2VFeAsO_3$ at $P = 0$, 1.9, and 2.4 GPa, respectively.

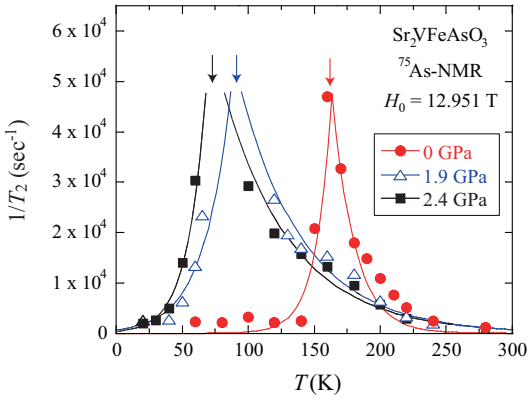

FIG. 5: (color online) The temperature dependence of $1/T_2$ at $P = 0$, 1.9, and 2.4 GPa, respectively. The curves are guides to the eyes. The arrows indicate T_N.

field, this result indicates that superconductivity coexists microscopically with antiferromagnetism. Previous NMR measurements on electron-doped $Ba(Fe_{1-x}Ni_x)_2As_2$[13] and hole-doped $Ba_{0.77}K_{0.23}Fe_2As_2$[25] found clear evidence for a microscopic coexistence of antiferromagnetism and superconductivity. However, in those compounds, the coexisting region is rather narrow and T_c there is lower than 20 K . In the present case, superconductivity is much more robust in the sense that the coexistence takes place in a wider parameter range and T_c is much higher (as high as 36.5 K) within the antiferromagnetically ordered phase.

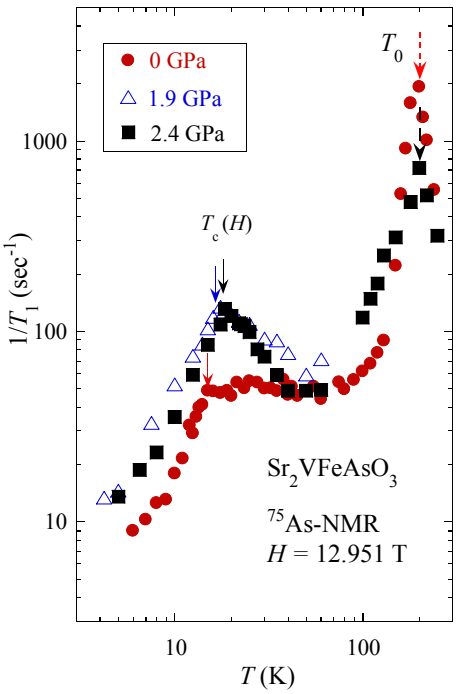

FIG. 6: (color online) The temperature dependence of $1/T_1$ at $P = 0$, 1.9, and 2.4 GPa obtained by As-NMR in the fixed magnetic field of 12.951 T. Solid arrows indicate $T_c(H)$.

IV. DISCUSSION

The electrical resistivity decreases with decreasing temperature and shows a further a sharper decreases at $T_0 \sim 200$ K.[18] As seen in Fig. 6, we found a peak at this T_0 in the T-dependence of $1/T_1$. The magnitude of the $1/T_1$ at T_0 is reduced by pressure, but T_0 is almost pressure independent. Since no internal magnetic field was found at this temperature, a magnetic cause may be excluded. The origin of T_0 is unknown at the present stage.

Finally, we show in Fig. 7 the pressure-temperature phase diagram for $Sr_2VFeAsO_3$ obtained from the present work. The T_N is reduced by pressure rapidly in a rate of -40 K/GPa. Concomitantly, T_c moderately increases in a ratio of 2 K/GPa. Qualitatively, the obtained phase diagram is similar to other iron pnictides.[5,13,25] However, $T_c = 36.5$ K is much higher than other systems in the region with a coexistence of antiferromagnetisim.

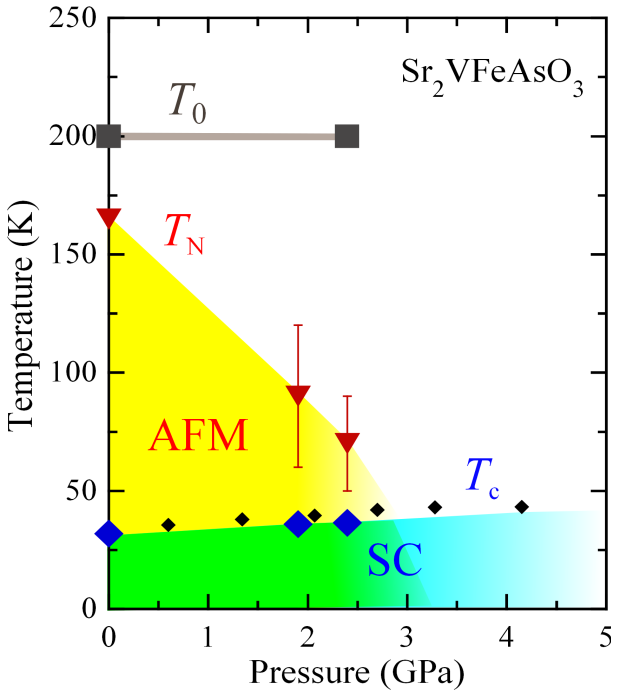

FIG. 7: (color online) The phase diagram for $Sr_2VFeAsO_3$ obtained by present work. The smaller solid diamonds are referred from the resistivity measurements.[19]

V. SUMMARY

We have performed ^{75}As- and ^{51}V-nuclear magnetic resonance (NMR) measurements on the iron-based superconductor $Sr_2VFeAsO_3$ with alternating stacks. We found an internal magnetic field at the As site, and a field distribution at the V site below $T_N = 165$ K, at which the ^{75}As nuclear spin-spin relaxation rate ($1/T_2$) shows a pronounced peak. We concluded that Fe electrons order antiferromagnetically with a magnetic moment $m_{Fe} \sim 0.4$ μ_B. Applying external pressure up to 2.4 GPa reduces T_N in a rate of -40 K/GPa, and enhances T_c in a rate of 2 K/GPa. The pressure-temperature phase diagram for $Sr_2VFeAsO_3$ shows that superconductivity coexists with antiferromagnetism with an unprecedented high T_c up to 36.5 K.

Acknowledgments

We thank S. Tsutsui and P. C. Dai for useful discussions. This work was supported in part by research grants from MEXT of Japan (No. 22103004 and 25400374) and from

MOST of China (973 project, No. 2011CBA00100 and 2012CB821402).

[1] Y. Kamihara, T. Watanabe, M. Hirano, and H. Hosono, J. Am. Chem. Soc. **130**, 3296 (2008).

[2] X. H. Chen, T. Wu, G. Wu, R. H. Liu, H. Chen, and D. F. Fang, Nature **453**, 761 (2008).

[3] Z.-A. Ren,W. Lu, J. Yang,W. Yi, X.-L. Shen, Z.-C. Li, G.-C. Che, X.-L. Dong, L.-L.Sun, F. Zhou, and Z.-X. Zhao, Chin. Phys. Lett. **25**, 2215 (2008).

[4] M. Rotter, M. Tegel, and D. Johrendt, Phys. Rev. Lett. **101**, 107006 (2008).

[5] A. S. Sefat, R. Jin, M. A. McGuire, B. C. Sales, D. J. Singh, and D. Mandrus, Phys. Rev. Lett. **101**, 117004 (2008).

[6] X. C. Wang, Q. Q. Liu, Y. X. Lv, W. B. Gao, L. X. Yang, R. C. Yu, F. Y. Li, and C. Q. Jin, Solid State Commun. **148**, 538 (2008).

[7] J. H. Tapp, Z. Tang, B. Lv, K. Sasmal, B. Lorenz, P. C. W. Chu, and A. M. Guloy, Phys. Rev. B **78**, 060505 (2008).

[8] F. C. Hsu, J. Y. Luo, K. W. Yeh, T. K. Chen, T. W. Huang, P. M. Wu, Y. C. Lee, Y. L. Huang, Y. Y. Chu, D. C. Yan, and M. K. Wu, Proc. Natl. Acad. Sci. **105**, 14262 (2008).

[9] J. Guo, S. Jin, G. Wang, S. Wang, K. Zhu, T. Zhou, M. He, and X. Chen, Phys. Rev. B **82**, 180520(R) (2010).

[10] T. Park, E. Park, H. Lee, T. Klimczuk, E. D. Bauer, F. Ronning, J. D. Thompson, J. Phys.: Condens. Matter. **20**, 322204, (2008).

[11] M. S. Torikachvili, S. L. Bud'ko, Ni Ni, and P. C. Canfield, Phys. Rev. Lett. **101**, 057006, (2008).

[12] P. L. Alireza, Y. T. Chris Ko, J. Gillett, C. M. Petrone, J. M. Cole, G. G. Lonzarich, S. E. Sebastian, J. Phys.: Condens. Matter. **21**, 12208 (2009).

[13] R. Zhou, Z. Li, J. Yang, D. L. Sun, C. T. Lin, G.-q. Zheng, Nat. Commun. **4**, 2265 (2013).

[14] F. L. Ning, K. Ahilan, T. Imai, A. S. Sefat, M. A. McGuire, B. C. Sales, D. Mandrus, P. Cheng, B. Shen, and H.-H Wen, Phys. Rev. Lett. **104**, 037001 (2010).

[15] T. Oka, Z. Li, S. Kawasaki, G. F. Chen, N. L. Wang, and G.-q. Zheng, Phys. Rev. Lett. **108**, 047001 (2012).

[16] Y. Nakai, T. Iye, S. Kitagawa, K. Ishida, H. Ikeda, S. Kasahara, H. Shishido, T. Shibauchi, Y. Matsuda, and T. Terashima, Phys. Rev. Lett. **105**, 107003 (2010).

[17] Z. Li, D. L. Sun, C. T. Lin, Y. H. Su, J. P. Hu, G.-q. Zheng, Phys. Rev. B **83**, 140506(R) (2011).

[18] X. Zhu, F. Han, G. Mu, P. Cheng, B. Shen, B. Zeng, and Hai-Hu Wen, Phys. Rev. B **79**, 220512 (R) (2009).

[19] H. Kotegawa, Y. Tao, H. Tou, H. Ogino, S. Horii, K. Kishio, J. Shimoyama, J. Phys. Soc. Jpn. **80**, 014712 (2011).

[20] H. Ogino, Y. Matsumura, Y. Katsura, K. Ushiyama, S. Horii, K. Kishio, and J. Shimoyama, Supercond. Sci. Technol. **22**,085001 (2009).

[21] S. Kakiya, K. Kudo, Y. Nishikubo, K. Oku, E. Nishibori, H. Sawa, T. Yamamoto, T. Nozaka, and M. Nohara, J. Phys. Soc. Jpn. **80**, 093704 (2011).

[22] G.H. Cao, Z. Ma, C. Wang, Y. Sun, J. Bao, S. Jiang, Y. Luo, C. Feng, Y. Zhou, Z. Xie, F. Hu, S. Wei, I. Nowik, I. Felner, L. Zhang, Z. Xu, and F.C Zhang, Phys. Rev. B **82**, 104518 (2010).

[23] M. Rotter, M. Tegel, D. Johrendt, I. Schellenberg, W. Hermes, and R. Pöttgen, Phys. Rev. B. **78**, 020503(R) (2008).

[24] H.-H. Klauss, H. Luetkens, R. Klingeler, C. Hess, F. J. Litterst, M. Kraken, M. M. Korshunov, I. Eremin, S.-L. Drechsler, R. Khasanov, A. Amato, J. Hamann-Borrero, N. Leps, A. Kondrat, G. Behr, J. Werner, and B. Büchner, Phys. Rev. Lett. **101**, 077005 (2008).

[25] Z. Li, R. Zhou, Y. Liu, D. L. Sun, J. Yang, C. T. Lin, and Guo-qing Zheng, Phys. Rev. B **86**, 180501(R) (2012).

[26] K. Matano, Z.A. Ren, X.L. Dong, L.L. Sun, Z.X. Zhao, Guo-qing Zheng, EPL **83**, 57001 (2008).

[27] Z. Li, Y. Ooe, X. C. Wang, Q. Q. Liu, C. Q. Jin, M. Ichioka, Guo-qing Zheng, J. Phys. Soc. Jpn. **79**, 083702 (2010).

[28] A. S. Kirichenko, A. V. Kornilov, V. M. Pudalov, Instrum. Exp. Tech. **48**, 121 (2005).

[29] S. Kawasaki, T. Tabuchi, X. F. Wang, X. H. Chen, Guo-qing Zheng, Supercond. Sci. Technol. **23**, 054004 (2010).

[30] A. Abragam: *The Principles of Nuclear Magnetism* (Oxford University Press, London, 1961).

[31] K. Kitagawa, N. Katayama, K. Ohgushi, M. Yoshida, M. Takigawa, J. Phys. Soc. Jpn. **77**, 114709 (2008).

[32] M. Yoshida, M. Takigawa, H. Yoshida, Y. Okamoto, and Z. Hiroi, Phys. Rev. Lett. **103**, 077207 (2009).

[33] Q. Huang, Y. Qiu, W. Bao, M. A. Green, J. W. Lynn, Y. C. Gasparovic, T. Wu, G. Wu, and X. H. Chen, Phys. Rev. Lett. **101**, 257003 (2008).

[34] de la Cruz C, Q. Huang, J. W. Lynn, Jiying Li, W. Ratcliff, J. L. Zarestky, H. A. Mook, G. F. Chen, J. L. Luo, N. L. Wang, and P. Dai, Nature **453**, 899 (2008).

[35] J. Munevar, D. R. Sánchez, M. Alzamora, E. Baggio-Saitovitch, J. P. Carlo, T. Goko, A. A. Aczel, T. J. Williams, G. M. Luke, Hai-Hu Wen, Xiyu Zhu, Fei Han, and Y. J. Uemura, Phys. Rev. B **84**, 024527 (2011).

[36] F. Hummel, Y. Su, A. Senyshyn, and D. Johrendt, Phys. Rev. B **88**, 144517 (2013).

[37] F. Han, X. Y. Zhu, G. Mu, P. Cheng, B. Shen, B. Zeng, and H. H. Wen, Sci. China, Ser. G **53**, 1202 (2010).

[38] K. Kitagawa, N. Katayama, H. Gotou, T. Yagi, K. Ohgushi, T. Matsumoto, Y. Uwatoko, and M. Takigawa, Phys. Rev. Lett. **103**, 257002 (2009).

[39] R. Khasanov, S. Sanna, G. Prando, Z. Shermadini, M. Bendele, A. Amato, P. Carretta, R. De Renzi, J. Karpinski, S. Katrych, H. Luetkens, and N. D. Zhigadlo, Phys. Rev. B **84**, 100501(R) (2011).